PSFC/JA-11-27

Effects of thermal expansion of crystal-lattice on x-ray imaging crystal spectrometers

L. Delgado-Aparicio[1], M. Bitter[1], Y. Podpaly[2], J. Rice[2], W. Burke[2], M. Sanchez del Rio[3], K. Hill[1], N. Pablant[1], P. Beiersdorfer[4], R. Bell[1], R. Feder[1], C. Gao[2], D. Johnson[1], S. G. Lee[5], E. Marmar[2], M. L. Reinke[2], S. Scott[1] and R. Wilson[1]

1 Princeton Plasma Physics Laboratory, Princeton, NJ, USA.
2 Massachusetts Institute of Technology, Cambridge, MA, USA.
3 European Synchrotron Radiation Facility, Grenoble, France.
4 Lawrence Livermore, National Laboratory, Livermore, CA, USA.
5 National Fusion Research Institute, Daejon, Korea

November 2011

Plasma Science and Fusion Center
Massachusetts Institute of Technology
Cambridge MA 02139 USA

This work was supported by US DoE awards DE-FC02-99ER54512 at MIT and DE-FC02-99ER54512 and DE-AC02-09CH11466 at PPPL and DE-AC52-07NA27344 at LLNL.

To be submitted for publication to Review of Scientific Instruments, 2011.

Effects of thermal expansion of crystal-lattice on x-ray imaging crystal spectrometers

L. Delgado-Aparicio[1*†], M. Bitter[1], Y. Podpaly[2], J. Rice[2], W. Burke[2], M. Sanchez del Rio[3], K. Hill[1], N. Pablant[1], P. Beiersdorfer[4], R. Bell[1], R. Feder[1], C. Gao[2], D. Johnson[1], S. G. Lee[5], E. Marmar[2], M. L. Reinke[2], S. Scott[1] and R. Wilson[1]

[1] Princeton Plasma Physics Laboratory, Princeton, New Jersey 08543, USA
[2] Massachusetts Institute of Technology - Plasma Science Fusion Center, Cambridge, Massachusetts 02139, USA
[3] European Synchrotron Radiation Facility, Grenoble, France
[4] Lawrence Livermore National Laboratory, Livermore, California 94550, USA
[5] National Fusion Research Institute, Daejon, Korea

December 8, 2011

Abstract

X-ray imaging crystal spectrometers with high spectral and spatial resolution are currently being used on magnetically confined fusion schemes to infer the time history of profiles of the ion and electron temperatures as well as plasma flow velocities. Recent studies indicate that the crystal temperature must be kept constant within a fraction of a degree to avoid changes of the interplanar $2d$-spacing by thermal expansion that cause changes in the Bragg angle, which could be misinterpreted as Doppler shifts. For the instrumental parameters of the x-ray crystal spectrometer on C-Mod, where those thermal effects were investigated, a change of the crystal temperature by one degree ^{o}C causes a change of the lattice spacing of the order of $\Delta d = 1 \times 10^{-5}$Å. This effect must also be considered for x-ray imaging crystals spectrometers installed on LHD, KSTAR, EAST, NSTX and, in the future, ITER.

*ldelgado@pppl.gov
†Presently at the Massachusetts Institute of Technology - Plasma Science Fusion Center.

1 Introduction.

High-resolution single-chord x-ray crystal spectrometers have been used to diagnose the core of tokamak plasmas for more than three decades (see ref. [1]-[2] and references therein). But thanks to the development of a new type of x-ray imaging crystal spectrometer which makes use of the imaging properties of spherically bent crystals [3]-[4], and due to important advances in the x-ray detector technology, especially, the manufacturing of two-dimensional pixilated x-ray detectors of large areas and high count rate capabilities [5], it is now possible to record spatially resolved x-ray spectra of highly charged ions from tokamak plasmas. These spectral data can be tomographically inverted to extract information on the local ion and electron temperatures ($T_{i,e}$) as well as toroidal and poloidal plasma flow velocity components ($v_{\phi,\theta}$). The ion temperature and flow measurements are based on measurements of the Doppler broadening and Doppler shift of the spectral lines, while the electron temperature is usually determined from the intensity ratios of the resonance line and the associated dielectronic satellites.

At the heart of the x-ray imaging crystal spectrometers is a spherically bent crystal, which serves as the x-ray diffracting element. This spherically bent crystal Bragg reflects x-ray radiation emitted from the plasma onto a two-dimensional, position-sensitive x-ray detector, such that the chord-integrated spectra from multiple sightlines are spatially resolved and observed simultaneously (see references [3]-[14]). The spectrometer resolving power can be as high $\lambda/d\lambda \sim 2 \times 10^4$ while the spatial and temporal resolutions are typically, about 1 cm and 5-20 ms, respectively. This new type of x-ray imaging crystal spectrometer is currently being used on several fusion devices, including the National Spherical Torus Experiment (NSTX, see ref. [3]) and Alcator C-Mod (see ref. [4]-[8]) in the USA, the Korean Superconducting Tokamak Advanced Reactor (KSTAR, see ref. [9]), the Experimental Advanced Superconducting Tokamak (EAST, see ref. [10]-[12]) in China, and the Large Helical Device (LHD, see ref. [11]) in Japan. This type of x-ray imaging crystal spectrometer has also been selected by the International Thermonuclear Experimental Reactor (ITER) organization to be a primary diagnostic for profile measurements of ion temperature (T_i) and toroidal velocity (v_ϕ), and to be a secondary diagnostic for electron temperature (T_e) and poloidal velocity (v_θ) [13]-[14]; at least four core-viewing spectrometers will be used in the near future at ITER.

The main objective of this paper is to investigate the long term thermal stability of this kind of crystal spectrometer in light of the harsh environment associated with a burning plasma in ITER; the dimensions and components of their future x-ray crystal imaging spectrometers (e.g. crystals, Bragg angles and x-ray detectors) will be very similar to those of the spectrometers presently used on C-Mod. This paper is organized as follows: The theoretically expected changes in crystal lattice spacing due to a thermal expansion of the crystal and resulting effects on wavelength measurements are described in Section 2. Experimental results from an investigation of these effects, using the x-ray imaging crystal spectrometer on C-Mod, are presented in Section 3; and implications for the ITER x-ray crystal spectrometers are discussed in Section 4.

2 Theoretical considerations.

The basic equation for wavelength measurements with an x-ray crystal spectrometer is the Bragg condition:

$$2d \sin\theta = \lambda \qquad (1)$$

where λ, d, and θ are the wavelength of an x-ray line, the interplanar spacing of the Bragg reflecting crys-

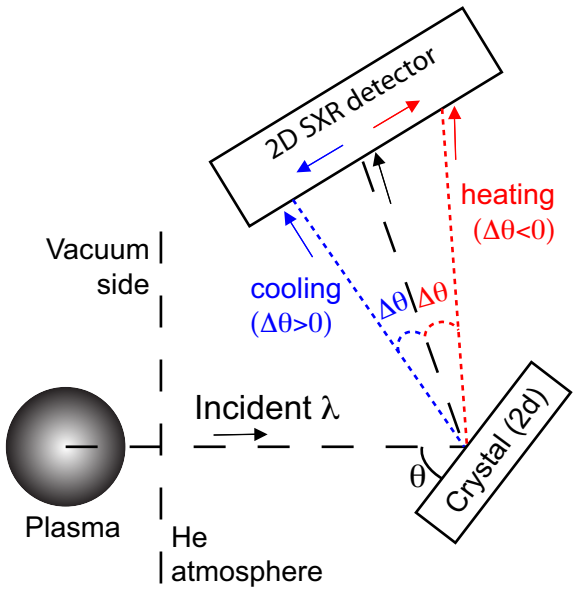

Figure 1: (Color-online) Variation of Bragg angle with change of $2d$ spacing as a result of thermal expansion assuming a constant wavelength λ (not to scale).

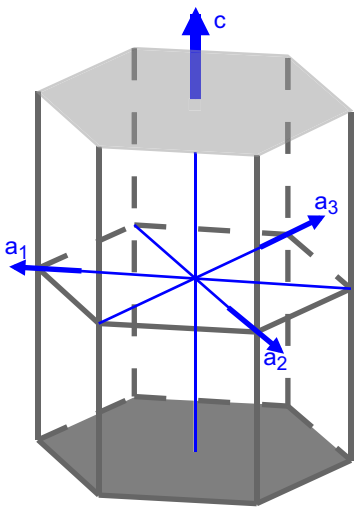

Figure 2: (Color-online) Hexagonal structure of quartz crystals used on Alcator C-Mod.

tal lattice planes, and the Bragg angle, respectively. One of the main tasks of the high resolution x-ray crystal spectrometers on tokamaks is to measure the velocity of an x-ray emitting ion from the observed wavelength shift (or Doppler shift) of a spectral line. The relationship between the Doppler shift, $\Delta\lambda$, and an ion velocity, v, is given by the Doppler equation:

$$\frac{\Delta\lambda}{\lambda} = \frac{v}{c} \tag{2}$$

From equation (1), we find - assuming that the lattice spacing, d, is constant - that the observed relative wavelength shift is given by

$$\frac{\Delta\lambda}{\lambda} = \frac{\Delta\theta}{\tan\theta} \tag{3}$$

On the other hand, we find from equation (1) that, for a constant wavelength, λ, a change, Δd, of the lattice spacing, e.g. by thermal expansion, leads to a change, $\Delta\theta$, of the observed of the Bragg angle, given by

$$\frac{\Delta d}{d} = -\frac{\Delta\theta}{\tan\theta} \tag{4}$$

The changes, $\Delta\theta$, expected for a heating or cooling of the crystal lattice are illustrated in Fig. 1. Comparing equations (3) and (4), one finds that the observed changes $\Delta\theta$ of the Bragg angle due to a relative wavelength shift, $\Delta\lambda/\lambda$, and a relative change of the crystal lattice spacing, $\Delta d/d$, which may result from a thermal expansion of the crystal, have exactly the same functional dependence. The changes of the Bragg angle due to these very different causes are, therefore, experimentally indistinguishable.

The relative changes of the crystal lattice spacing by thermal expansion are given by

$$\frac{\Delta d}{d} = \alpha_{eff} \cdot \Delta T \tag{5}$$

where, ΔT is the change in temperature and α_{eff} is an effective thermal expansion coefficient of the crystal which will be explained below. According to equations (3)-(5) and Figure 1, the expansion of the crystal due to an increases in temperature of $\Delta T > 0$ will result in a change $\Delta\theta < 0$. This effect can easily be misinterpreted as a Doppler shift if the temperature variations of the crystal and its thermal expansion are unknown. Since the high-resolution crystal spectrometers on Alcator C-Mod as well as other tokamaks are designed to measure plasma flow velocities as low as 5-10 km/s, the minimum still observable Doppler shifts $\Delta\lambda/\lambda$ must be of the order of 1×10^{-5}. Thus it follows from equations (3) and (4) that errors due to the relative changes of the crystal lattice spacing $\Delta d/d$ must be less than 10^{-5}. Therefore, for our quartz crystals with $d = 2.28112$Å, the d-spacing must be kept constant to within 2×10^{-5}Å.

The crystals most commonly used in x-ray spectrometers on tokamaks, are quartz crystals which have a hexagonal lattice structure. The interplanar $2d$-spacing is given by [15],

$$\left|r^*_{h,k,l}\right|^{hex} = \frac{1}{d^{hex}_{h,k,l}} = \sqrt{\frac{4}{3a_0^2}\left[h^2+k^2+hk\right] + \frac{l^2}{c_0^2}} \tag{6}$$

where, (h,k,l) are the Miller indices, and $a_0 = 4913.04$ mÅ and $c_0 = 5404.63$ mÅ are the lattice constants at

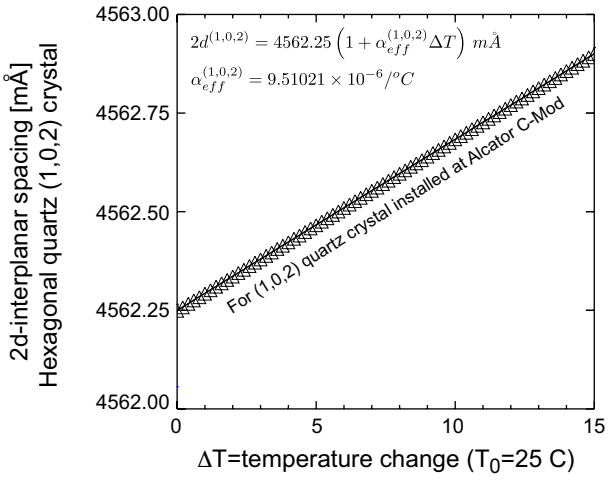

Figure 3: $2d$-interplanar spacing as a function of temperature change (ΔT) for the $(1,0,2)$-quartz crystal used at Alcator C-Mod.

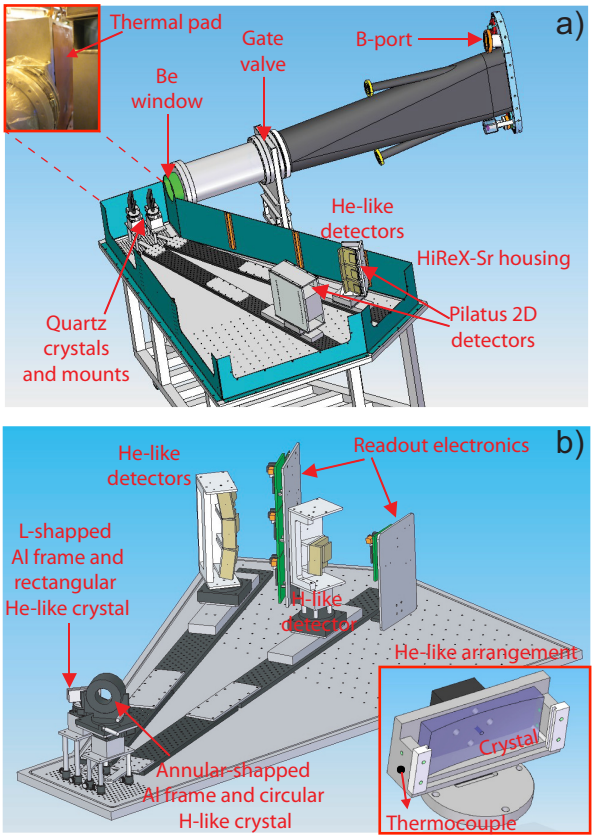

Figure 4: (Color-online) Schematic views of HiReX-Sr spectrometer installed in Alcator C-Mod. a) The thermal pad used in the temperature-scan was placed on the outside wall next to the two quartz crystal mounts. b) The L- and annular-shaped aluminum frames support the glass substrates that hold the rectangular and circular He- and H-like crystals, respectively.

25^{o}C of the crystal unit cell as shown in Figure 2 [15]-[16]. Materials with anisotropic structures, such as quartz, have distinct thermal expansion coefficients in different directions. For quartz crystals the thermal expansion coefficients are $\alpha_{\parallel} = 7.97 \times 10^{-6o}\mathrm{C}^{-1}$ and $\alpha_{\perp} = 13.37 \times 10^{-6}\mathrm{C}^{-1}$ in the directions parallel to the c_0 and a_0, respectively [15]-[16]. The unit cell values may change from crystal to crystal and from reference to reference (e.g. synthetic quartz vs. natural quartz), which actually sheds light on the importance of having a crystal characterization and calibration prior to its installation and use. The lattice spacing for a given temperature excursion ΔT is therefore given by:

$$d^{hex}_{h,k,l}(T) = \left(\frac{4\left[h^2 + k^2 + hk\right]}{3a_0^2(1+\alpha_{\perp}\Delta T)^2} + \frac{l^2/c_0^2}{(1+\alpha_{\parallel}\Delta T)^2} \right)^{-1/2} \quad (7)$$

A plot of the $2d$-spacing versus temperature excursion (ΔT) using equation (7) is shown in Figure 3 for the quartz crystal cut with Miller indices $(1, 0, 2)$ used at C-Mod. This function is well approximated by the linear expression: $[2d]\,(T) = [2d]_0\,(1 + \alpha_{eff}\Delta T)$ with an effective thermal expansion coefficient, $\alpha_{eff} = 9.51021 \times 10^{-6}/^o\mathrm{C}$.

3 Experimental results.

Measurements of $\Delta d/d$ as a function of temperature of the crystal were made by heating the outer wall of the spectrometer housing with a single thermal-pad as shown in the top-left insert of Figure 4-a). The thermal pad was located behind the crystals to selectively increase their temperature, and at the same time, minimize the temperature excursion of the other components installed throughout the spectrometer housing; this temperature measurements were done with two K-type thermocouples [17]. One probe was attached to the mount of the first crystal, which is used for measurements of He-like argon spectra and which is next to the heat source as shown in the bottom-right insert of Figure 4-b), while the second thermocouple was installed in between the crystals and the x-ray detectors (at the center of the spectrometer

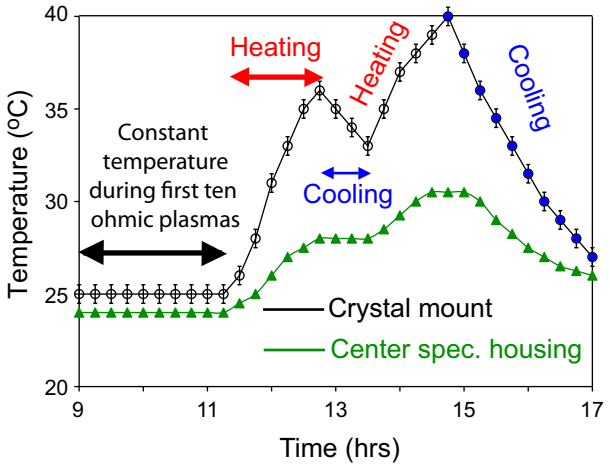

Figure 5: (Color-online) Time history of the temperature of the crystal mount during the heating and cooling phases.

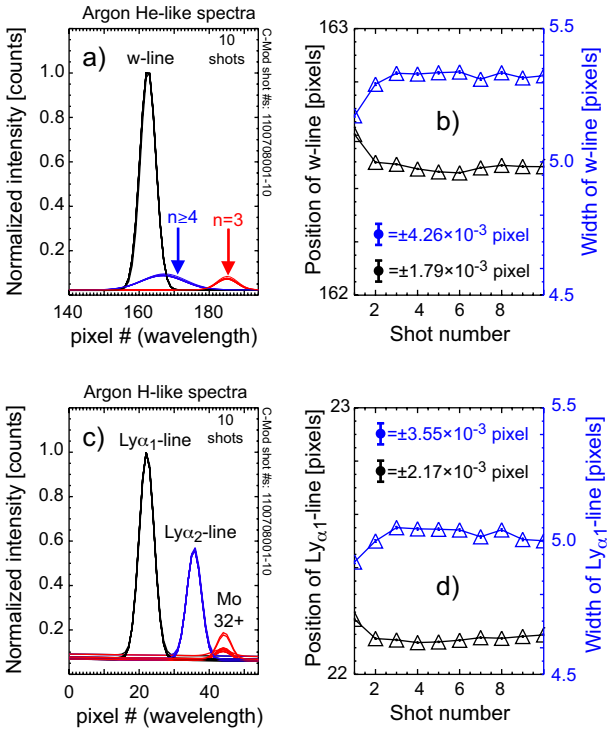

Figure 6: (Color-online) Overlay of He- and H-like argon spectra from 10-shots indicating high reproducibility of the spectral line positions during ohmic plasma conditions. The error bars from the multi-gaussian non-linear least-squares fit are well inside the data plot symbols and of the order of 10^{-3} pixels.

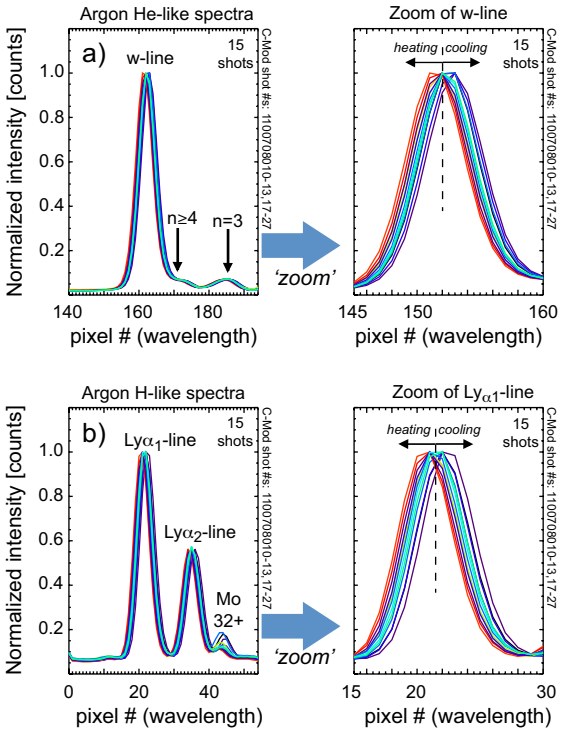

Figure 7: (Color-online) Overlay of spectral data from 15 shots during the temperature scan showing line shifts observed during the heating and cooling phases.

housing). The spectrometer chamber was filled with a helium atmosphere at $\sim$ 1 atm pressure to avoid attenuation in air of the low energy ($\sim 3-4$ keV) x-rays of the observed argon spectra. The time histories of the temperature measurements obtained during a work day are shown in Figure 5. At the beginning of the experiment the spectrometer housing was kept at a constant room temperature of 25^{o}C (see Figure 5) and the exact positions of the spectral lines on the detector were determined by using ten consecutive and reproducible ohmic discharges. The temperature of the heating pad was then set to 80^{o}C using a remotely adjusted temperature controller. As is evident from Figure 5, the time-constant for the observed temperature rise in the crystal mount is of the order of 1 hr, contrary to that of the thermal pad which was of only 2-4 minutes. The heating phase was interrupted in order to secure the integrity of the crystal during a temporal malfunction of the magnetic coils of Alcator C-Mod, causing a drop in the temperature of the crystal mount shown in Figure 5. The experimental conditions were later restored and the heating process begun after one hour. The heating was terminated when the crystal mount reached 40 ^{o}C which is the maximum operating temperature for the Pilatus detectors; the temperature excursion at the center of the spectrometer housing was less than 6 ^{o}C so we estimate a temperature increase of the detectors of only 1-2 ^{o}C. The measurements of the line positions were continued during the cooling process. Although the data were collected through several hours, we decided to base our conclusions on the data gathered during this last cooling period which was not interrupted by any impairments of the machine operation [see blue symbols in Figure 5 and Figures 8-a), b) and c)]. An overlay of the multi-gaussian fits of the resonance line "w" and its associated dielectronic satellites, as well as the Lyman-α doublet and the neon-like molybdenum line (Mo^{32+}) - which falls next to the Lyman-α doublet, are shown in Figures 6 and 7. The latter spectra were simultaneously recorded with the second crystal in our spectrometer.

The pixel size on our detector is 172 μm. However, the Doppler-broadened line spreads over

$\sim$10 pixels, so that it is possible to determined the position of the line with an accuracy much better that the pixel size. The line intensities, widths and centroid locations for the initial 10 consecutive shots did not change on a shot-to-shot basis (see Figs. 6) and were within the small error bars of (1.8-2.2)$\times 10^{-3}$ and (3.5-4.3)$\times 10^{-3}$ pixels, for the centroid position and line-width, respectively. The centroid positions, given in pixel numbers, for lines "w", Lyman-α_1 and Lyman-α_2 at 25^{o}C are $\sim$162.45, $\sim$22.15 and $\sim$35.7 in pixel, respectively.

The same ohmic plasma conditions were used throughout the entire experiment. An overlay of the raw data showing the spectral features during the heating and cooling phases is depicted in Figure 7. Shifts of the centroid positions, as expected for the heating and cooling phases from the discussion that followed Figure 1, are already evident from these raw data. The changes in the measured centroid of the lines as a function of temperature are shown in Figure 8, where the two distinct branches correspond to the heating and cooling phases. The data inferred from the w-line and the Lyman-α doublet for the cooling process from 38 to 26 ^{o}C is summarized in Tables 1 and 2; R_c is the radius of curvature of the crystal, while Δp is the experimentally inferred pixel shift and ds is the length of the arc subtended by the change $\Delta\theta$ in the Bragg angle due to the shrinkage of the $2d$-spacing. The values of $\Delta d/d$ inferred from the observed centroid shifts of the lines w and Lyman-α doublet, listed in Tables 1 and 2 are 8.02×10^{-5}, 12.59×10^{-5} and 12.47×10^{-5}, respectively. On the other hand, the theoretically expected value of $\Delta d/d$ according to equation (5) is 11.2×10^{-5} for the measured change in crystal mount temperature of 11.8^{o}C. The experimental data are therefore in reasonable agreement with our theoretical prediction.

In the following we compare the effects of the thermal expansion of the crystal lattice with those produced by a thermal expansion of the metallic spectrometer housing, especially, the change of the distance between the crystals and the SXR detectors. The thermal expansion of the crystal lattice, for an increase of the crystal temperature by as much as 10 ^{o}C, has two effects: It causes (a) a shift of the w-line on the detector of the order of 1 pixel and shifts of similar magnitude for all the observed spectral lines, and (b) it reduces the separation between the w-line and the z-line on the detector (at the other end of the He-like Ar spectrum) by approximately 10 microns. Of these two effects (a) is by far the most significant. A change of the crystal-detector distance by thermal expansion will primarily change the separation between w- and z-lines and to a much lesser extent cause a shift of the entire spectrum, so that

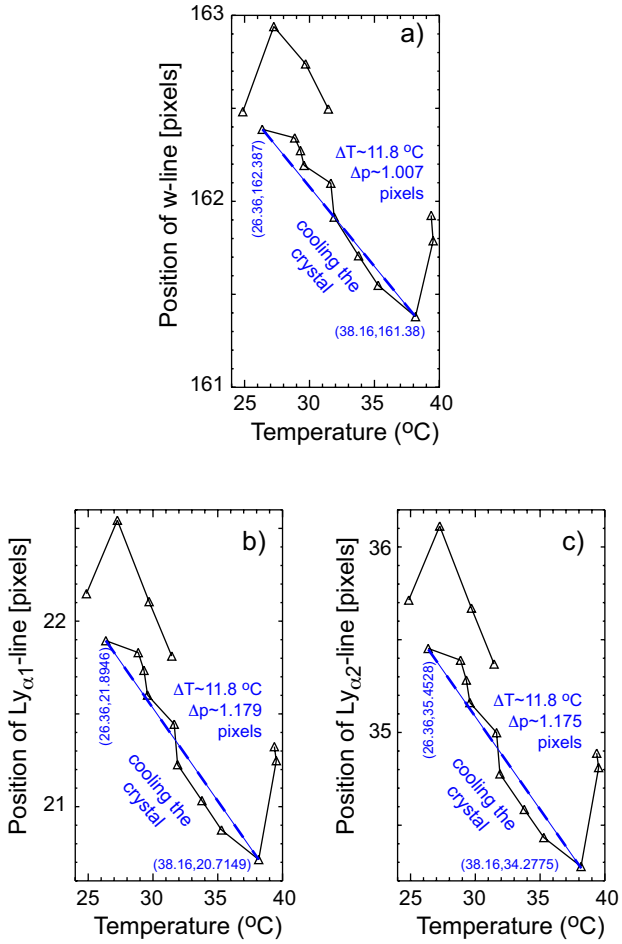

Figure 8: (Color-online) Line-shifts from temperature-dependent changes of $2d$-spacing.

Parameters	He-like ($w-$line)
λ (Å)	3.9492
$\theta_B = \sin^{-1}(\lambda/2d)$	59.9542^o
R_c (mm)	1443
$R_c \sin\theta_B$	1249.10
Δp (pixels)	1.007
$ds = \Delta p \times 0.172$	0.1732 mm
$\Delta\theta_B \approx \frac{ds}{R_c \sin\theta_B}$	1.387×10^{-4}
$\frac{\Delta d}{d} = -\frac{\Delta\theta_B}{\tan\theta_B}$	8.02×10^{-5}

Table 1: Spectroscopically measured parameters from the w-line of the He-like spectrometer used in Alcator C-Mod. The $(1,0,2)$ quartz crystals have a $2d$-spacing of the order of 4562.25 mÅ at 25 ^{o}C.

Parameters	$\mathrm{Ly}_{\alpha,1}$	$\mathrm{Ly}_{\alpha,2}$
λ (Å)	3.7311	3.7365
$\theta_B = \sin^{-1}(\lambda/2d)$	54.8671^o	54.9852^o
R_c (mm)	1385	1385
$R_c \sin\theta_B$	1132.68	1134.32
Δp (pixels)	1.179	1.175
$ds = \Delta p \times 0.172$	0.2028 mm	0.2021
$\Delta\theta_B \approx \frac{ds}{R_c \sin\theta_B}$	1.79×10^{-4}	1.781×10^{-4}
$\frac{\Delta d}{d} = -\frac{\Delta\theta_B}{\tan\theta_B}$	12.59×10^{-5}	12.47×10^{-5}

Table 2: Spectroscopically measured parameters from the H-like spectrometer used in Alcator C-Mod. The $(1, 0, 2)$ quartz crystals have a $2d$-spacing of the order of 4562.25 mÅ at 25 ^{o}C.

with respect to line shifts caused by a change of the crystal-detector distance effect (b) is much more significant than effect (a). In order to reduce the separation between the w- and z-lines on the detector by the same amount of 10 microns, it would be necessary to change the crystal-detector distance of the C-Mod spectrometer by 0.5 mm, which based on the thermal expansion coefficient of 16.7×10^{-6} /^{o}C for steel would require to reduce the temperature of the spectrometer housing by ~ 25 ^{o}C.

4 Implications for ITER

The edge and core x-ray imaging crystal spectrometers to be built for the International Thermonuclear Experimental Reactor (ITER) will have radial and partially tangential views to measure toroidal and poloidal velocities in the range from 1-100 km/s for a normalized radius of $r/a < 0.9$. According to the original specifications, the toroidal and poloidal velocities should both be measured with an accuracy below 30% [18]. For a typical core toroidal rotation measurement of the order of several tens to 100-200 km/s, the overall profile accuracy should be better than 10 km/s. A change of the temperature of the germanium crystals, which are presently being considered for the ITER spectrometers, by 1.0 degree ^{o}C would result in a $\Delta d/d$ that is four times larger than that observed on C-Mod due to the fact that the typical thermal expansion coefficient for germanium is $\alpha_{eff} = 36 \times 10^{-6}/^o$C, so that the observed change in Bragg angle could be mistaken as a Doppler shift which corresponds to a velocity of 10 km/s. The measurements of the toroidal rotation for the outer plasma ($r/a \sim 0.5 - 0.9$) will have an accuracy limited not only by signal-to-noise ratio constraints but also by the effect of changing the crystal temperature as discussed above. For a poloidal rotation measurement, with velocities typically an order of magnitude smaller, the problem is even more difficult. A peak poloidal velocity of 10-20 km/s implies a measurement accuracy that requires the crystal temperature excursion be smaller than 1/5 of a degree ^{o}C. Because the ITER spectrometer housing is kept at a constant temperature throughout the plasma shots, temperature excursions and spurious drifts in the inferred velocity estimates would likely arise from the x-ray flux heating the crystal surface.

In summary, the thermal excursion of the crystals used in x-ray imaging spectrometers can affect the $2d$ interplanar spacing introducing changes in the Bragg angle that can be experimentally misinterpreted as Doppler shifts; such thermal drifts can be due to non-reproducible and varying ambient temperatures and possibly to the x-ray flux impinging on the crystal. It is therefore imperative to monitor the time-history of the crystal temperature with an accuracy better than one degree. This work was performed under US DoE contracts DE-FC02-99ER54512 at MIT, DE-AC02-09CH11466 at PPPL and DE-AC52-07NA27344 at LLNL.

References

[1] M. Bitter, *et al.*, Can. J. Phys., **86**, 291, (2008).

[2] B. C. Stratton, *et al.*, Fusion Science and Technology, **53**, 431, (2008).

[3] M. Bitter, *et al.*, Rev. Sci. Instrum., **70**, 292, (1999).

[4] M. Bitter, *et al.*, Rev. Sci. Instrum., **75**, 3660, (2004).

[5] See for instance DECTRIS website at: http://www.dectris.ch/sites/products.html

[6] A. Ince-Cushman, *Rotation Studies in Fusion Plasmas via Imaging X-ray Crystal Spectroscopy*, Ph. D. thesis, MIT, (2008).

[7] A. Ince-Cushman, *et al.*, Rev. Sci. Instrum. **79**, 10E302, (2008).

[8] K. W. Hill, *et al.*, Rev. Sci. Instrum., **79**, 10E320, (2008).

[9] S. G. Lee, *et al.*, Rev. Sci. Instrum., **81**, 10E506, (2010).

[10] Y. Shi, *et al.*, Plasma Phys. Control. Fusion, **52**, 085014, (2010).

[11] M. Bitter, *et al.*, PPPL report 2514, (2010).

[12] N. Pablant, private communication, (2011). To be submitted to Rev. Sci. Instrum., (2011).

[13] K. W. Hill, *et al.*, Rev. Sci. Instrum., **81**, 10E322, (2010).

[14] P. Beiersdorfer, *et al.*, J. Phys. B: At. Mol. Opt. Phys., **43**, 144008, (2010).

[15] B. E. Warren, *X-ray difraction*, Dover, NY, (1990).

[16] R. W. G. Wyckoff, *Crystal structures*, 2nd edition, Vol. 1, John Wiley, (1963).

[17] L. Delgado-Aparicio, *et al.*, 52^{nd} Annual Meeting of the APS Division of Plasma Physics, Volume 55, Number 15, November 8-12, 2010.

[18] A. J. H. Donne, *et al.*, Nucl. Fusion, **47**, S337-S384, (2007).